A Phase-Shift Controlled Bi-directional DC-DC Converter

H. L. Chan, K. W. E. Cheng and D. Sutanto
The Hong Kong Polytechnic University,
Hung Hom, Hong Kong,
Tel: (852) 2766-6162

Abstract–**The newly developed phase-shift controlled bi-directional DC-DC converter has the conventional features of phase-shifted converters, including zero-voltage switching (ZVS) and constant switching frequency. However, it has been improved by developing a bi-directional power flow capability and applying synchronous rectification, hence the on-state voltage drop of the active devices are small.**

I. INTRODUCTION

The conventional bi-directional DC-DC converters [1-4] are most suitable for high voltage and high power applications. However the proposed converter [5] has been improved with bi-directional power flow, it is especially useful for regenerative braking in electric vehicle (EV), where the mechanical energy is converted into electrical energy by traction motor and then fed back into the EV batteries. The converter employs the phase shift technique for voltage control; utilizes parasitic capacitance of active switches and leakage inductance of transformer for resonant switching; does not require a large filter inductor and applies the synchronous rectification [6-7] for bi-directional power flow.

The bi-directional phase-shifted DC-DC converter is comprised of an inverter bridge (Q_1-Q_4) and a converter bridge (M_1-M_4), which are connected with a high frequency power transformer. The 50% duty-ratio gate signals applied to the converter bridge are synchronized with those applied to the inverter bridge. Fig. 1 shows the topology of the proposed converter. All the active switches in both the inverter and converter bridges are identical, each of them consists of a MOSFET with a body diode and a capacitor. The capacitors, C_1-C_4, represent the sum of stray capacitance of the MOSFET and an additional resonant capacitor. L_{lk} is the total leakage inductance of the transformer's primary and secondary windings. C_{in} and C_{out} are the input and output filter capacitors. V_{in} and V_{out} are the input and output voltage. $i(t)$ is the primary current of transformer.

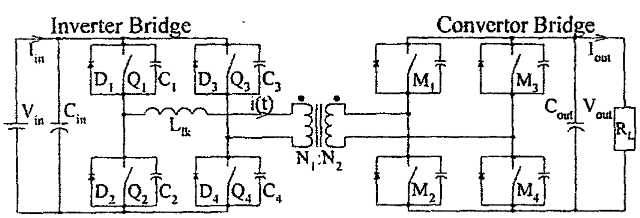

Fig. 1. Bi-directional Phase-Shifted DC-DC Converter

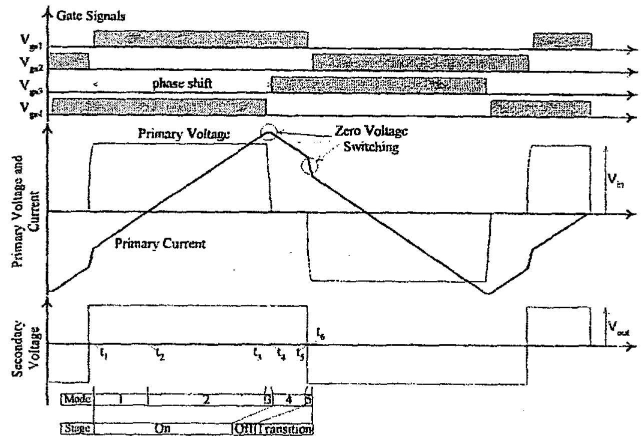

Fig. 2. Idealised Voltage and Current Waveforms

The complete cycle of operation for the bi-directional phase-shifted DC-DC converter is shown in Fig. 2. V_{gs1} to V_{gs4} are gate signals applied to Q_1 to Q_4. In addition, V_{gs1} is also used to drive M_1 and M_4, V_{gs2} to drive M_2 and M_3, such that the converter bridge can operate in the manner of synchronous rectification. The synchronous rectification allows the converter to have low on-state loss and ease of control at the transistors M_1 to M_4.

II. OPERATIONS OF THE CIRCUIT

The circuit operation in positive half cycle is the same as the negative half cycle except the signs of voltage and current are reversed, so only the positive half cycle is explained here. The operation principle can be divided into five modes.

1) *Mode 1*: Q_1 and Q_4 are on. V_{in} is applied across the primary winding of transformer, and the secondary winding of transformer is clamped to V_{out} as M_1 and M_4 are on. As energy has been stored in L_{lk} during the previous mode of operation, then the primary current $i(t)$ flows in reverse direction.

2) *Mode 2*: When energy in L_{lk} is empty, the source is supplying energy to the load, and $i(t)$ flows in forward direction.

3) *Mode 3*: Q_1 remains on, but Q_4 is being turned off. Energy in L_{lk} is charging up C_4 and discharging C_3 simultaneously. D_3 will conduct once the voltage across C_3 is

0-7803-5491-5/99/$10.00 © 1999 IEEE

zero. Subsequently, Q_3 is turned on under zero voltage switching (ZVS). It is clear that a dead time between turn-off of Q_4 and turn-on of Q_3 is needed for Q_3 to achieve the ZVS.

$$\text{Dead time, } \delta_3 \frac{T}{2} = \frac{V_{in} C_{right}}{I_3} \tag{1}$$

where C_{right} is sum of C_3, C_4 and stray capacitance of transformer winding.

4) *Mode 4*: Q_1 and Q_3 are on. Energy in L_{lk} continues to deliver to the load, and the large output filter capacitor maintains the secondary of transformer at V_{out}.

5) *Mode 5*: Q_3 remains on, but Q_1 is being turned off. C_1 is being charged up and C_2 is being discharged simultaneously by the energy in L_{lk}. Once voltage across C_2 reaches zero, D_2 conducts and Q_2 switches on under ZVS condition. Also a dead time between the turn-off of Q_1 and turn-on of Q_2 is required for ZVS of Q_2.

$$\text{Dead time, } \delta_5 \frac{T}{2} = \sqrt{L_{lk} C_{left}} \tan^{-1}\left(\frac{I_5}{n V_{out}} \sqrt{\frac{L_{lk}}{C_{left}}} \right) \tag{2}$$

where C_{left} is sum of C_1, C_2 and stray capacitance of transformer winding.

Furthermore, there is a minimum load requirement for the converter to achieve ZVS, it is given in (3).

$$i(t_5) \geq \sqrt{\frac{C_{left}}{L_{lk}} V_{in} \left(V_{in} + 2nV_{out} \right)} \tag{3}$$

III. MATHEMATICAL CALCULATIONS

The voltage conversion ratio and control region were calculated with the parameters: D = phase shift, n = turn ratio, T = switching period. In addition, C_{out} is assumed to be sufficiently large to hold V_{out} at nearly constant. Three states are defined as follows:

A. Voltage Conversion Ratio

1) "*On*" *Stage* ($t_1 < t \leq t_4$) or ($t_4 - t_1 = DT/2$): Since modes 1 and 2 are identical when they are considered under circuit theory, and the primary current changes in mode 3 is small, so this stage includes modes 1, 2 and 3. In addition, we also neglect the dead time $\delta_3 T/2$ as it is insignificant when compared with D. The circuit equation describing the "On" stage is,

$$V_{in} - nV_{out} = L_{lk} \frac{di}{dt} \tag{4}$$

2) "*Off*" *Stage* ($t_4 < t \leq t_5$) or $t_5 - t_4 = (1 - D - \delta_5)T/2$: This stage is exactly the mode 4 of operation, energy in L_{lk} is freewheeling to drive the load, and (5) is the circuit equation.

$$-nV_{out} = L_{lk} \frac{di}{dt} \tag{5}$$

3) "*Transition*" *Stage* ($t_5 < t \leq t_6$) or $t_6 - t_5 = \delta_5 T/2$: This stage is the changeover of the "Off" stage to the "On" stage, it is actually the mode 5 of operation. Circuit equation of this stage is given in (6).

$$-V_{in} - nV_{out} = L_{lk} \frac{di}{dt} \tag{6}$$

The input energy W_{in} to the converter during a half cycle is:

$$W_{in} = \int_0^{DT/2} i(t) \cdot V_{in} \cdot dt. \tag{7}$$

Then, solving (4), (5), (6) and (7), we got

$$W_{in} = \left(\frac{V_{in}\delta_5 T + (1-D) nV_{out} T}{2L_{lk}} \right) V_{in} D \frac{T}{4} \tag{8}$$

And the output energy W_{out} for a half cycle is given by:

$$W_{out} = \frac{T}{2} \cdot \frac{V_{out}^{\ 2}}{R_{Load}} \tag{9}$$

Assumed that $W_{out} = W_{in}$, we obtained

$$\left(\frac{V_{out}}{V_{in}} \right)^2 - nkD(1-D)\left(\frac{V_{out}}{V_{in}} \right) - k\delta_5 D = 0, \tag{10}$$

where $k = \frac{R_{Load} T}{4L_{lk}}$. This is the DC characteristic of the converter.

B. Maximum and Minimum Phase Shift

1) *Maximum Phase Shift* (D_{max}): The maximum output voltage, when phase shift = D_{max}, can be obtained by differentiating (10) with respect to D, and D_{max} is given in (11).

$$D_{max} = \frac{nV_{out} + \delta_5 V_{in}}{2nV_{out}} \tag{11}$$

2) *Minimum Phase Shift* (D_{min}): The minimum load current $i(t_5)$ in terms of phase shift can be derived from (4), (5) and (6), and it is substituted in (3) to yield D_{min}.

$$D_{min} \geq \frac{4\sqrt{C_{left} L_{lk}}}{T}\sqrt{1+2\frac{nV_{out}}{V_{in}}}+\frac{nV_{out}}{V_{in}} \quad (12)$$

C. Control Region

Plotting (10), (11) and (12) on the same graph, we get Fig. 3, which shows the optimal control region of the converter. This graph can then be used for design of the proposed converter.

IV. EXPERIMENTS

There were two experiments carried out to test the performance of the proposed converter's efficiency and reverse mode of operation.

A. Experiment One – Conversion Efficiencies

A prototype of the proposed converter was built up with the specifications: switching frequency of 100kHz, input voltage of 70V and output voltage of 30V. The circuit components included: all of MOSFETs (Q_1-Q_4 and M_1-M_4) are IRF530N, L_{lk} is 21.8μH, C_1-C_4 are 3.2nF, C_{in} and C_{out} are 5.4μF and 14.8μF respectively. Moreover, the power transformer was constructed using a bobbin of ETD49 and Ferrite core material of 3C85, its turn number of primary winding (N_1) and secondary winding (N_2) were 70 and 40 respectively.

Under the load range from 60W to 120W, the conversion efficiencies were measured and plotted in Fig. 4. It is obvious that the overall efficiency of the proposed converter is more than 91% over the specific load range.

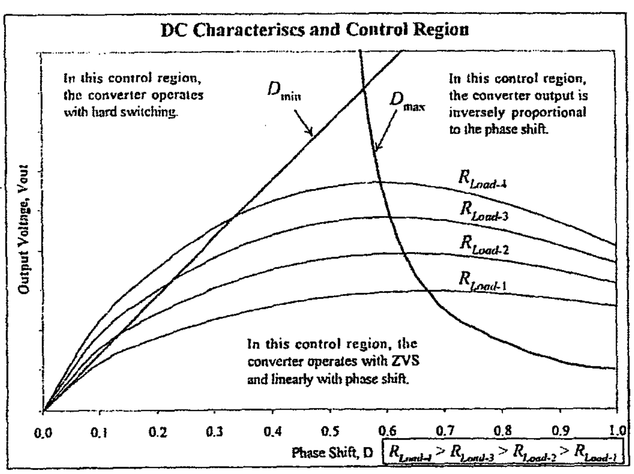

Fig. 3. Converter Efficiencies

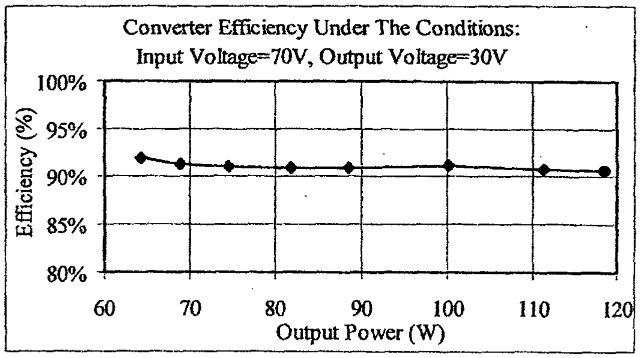

Fig. 4. Converter Efficiencies

Investigating the switching of MOSFET as shown in Fig. 5 can support the high conversion efficiency.

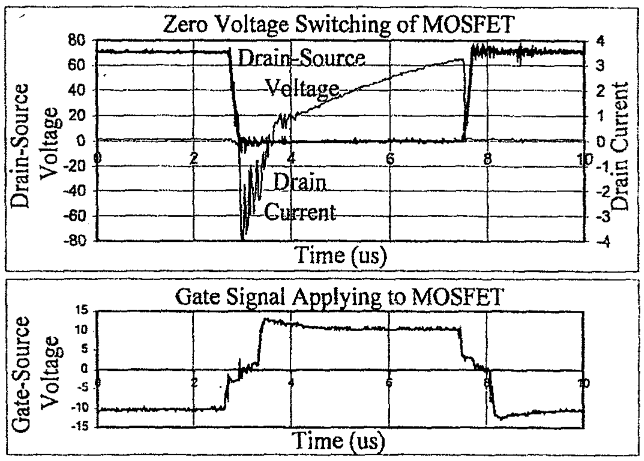

Fig. 5. Zero–Voltage Switching of MOSFET Q_4

It was clearly shown that the drain-source voltage of Q_4 has been resonated to zero before the gate-source signal is applied. With the aim of this switching method, the switching losses of MOSFETs are minimized, and the overall efficiency of the converter is maximized. The other MOSFET switching waveforms are similar.

B. Experiment Two – Reverse Operation

Another experimental setup shown in Fig. 6 was used to test the performance of bi-directional power flow of the converter, where the converter input was connected to 70V batteries and the converter output was connected to the load and a switch in series with an external power supply of 45V.

When the switch remains opened, the converter operates in forward mode, and it will change in reverse mode once the switch is closed.

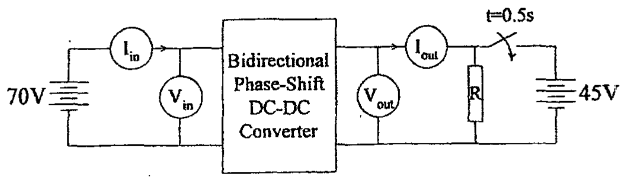

Fig. 6. Experiment for Reverse Operation

Initially, the converter ran with V_{in} = 70V, I_{in} = 1.08A, V_{out} = 36V and I_{out} = 1.95A. When t = 0.5s, the external voltage source of 45V was applied momentarily to the output of the converter. The output current and input current flowed in reverse direction simultaneously with amplitude of 1.9A and 1.1A respectively, however, the input voltage almost kept constant at 70V either in forward and reverse operations. Fig. 7 shows the changeover of operations.

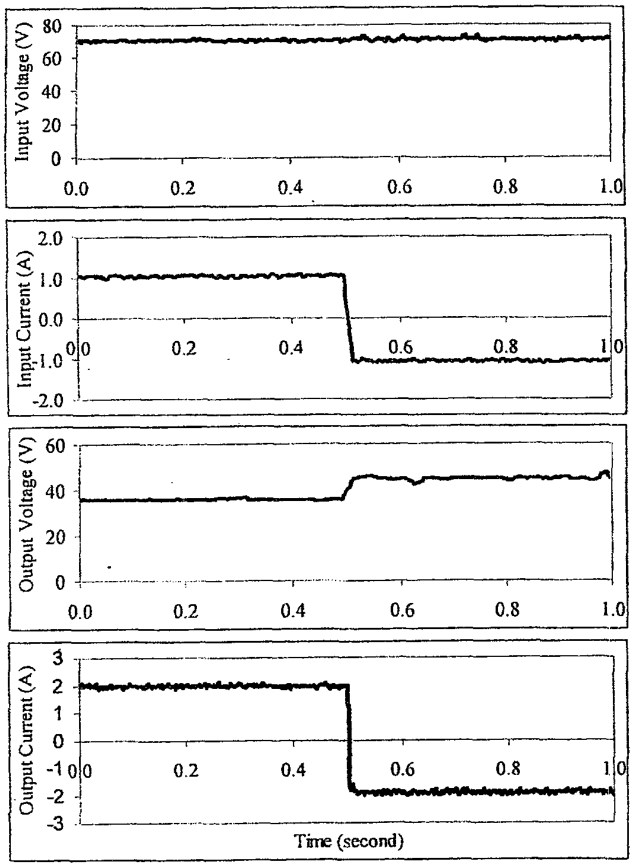

Fig. 7. Changeover from forward to reverse power flow operations

V. CONCLUSION

A novel bi-directional phase-shift controlled DC-DC converter was proposed. The converter uses leakage inductance of the transformer and parasitic capacitance of active switches to perform resonant switching. All the active switching devices are switched at zero voltage switching. The proposed converter, if employed in EV, is capable of not only transferring energy from EV batteries to powertrain for motoring, but also returning energy back into batteries in case of regenerative braking.

Moreover, by making use of a simple drive circuit for the converter bridge, it can gain the benefit of synchronous rectification.

ACKNOWLEDGEMENTS

This project is supported and funded by The Hong Kong Polytechnic University, and the project account code is G-V305.

REFERENCES

[1] Forsyth A.J., Evans P.D., Cheng K.W.E. and Ai-Mothafar M.R.D., "Operation Limits Of Power Converters For High Power Ion Engine Control", *AIDAA/AIAA/DGLR/JSASS 22nd Int'l Electric Propulsion Conf.*, 1991.

[2] Forsyth A.J., Evans P.D., Ai-Mothafar M.R.D. and Cheng K.W.E., "A Comparison Of Phase-Shift Controlled Resonant And Square-Wave Converters For High Power Ion Engine Control", *Proc. Of the European Space Power Conf.*, 1991.

[3] Vlatkovic V., Ridley, Lee F. C. and Cho B. H., "Design Consideration For High Voltage, High Power, Full Bridge, Zero Voltage Switched PWM Converter", *Proc. of the IEEE APEC.*, 1990, pp. 275-284.

[4] Cho J. G., Sabate J. A., Hua G. and Lee F. C., "Zero-Voltage And Zero-Current-Switching Full Bridge PWM Converter For High-Power Applications", *IEEE Trans. On Power Electronics*, Vol. 11, No. 4, July, 1996. pp. 622-628.

[5] H. L. Chan, K. W. E. Cheng and D. Sutanto, "Bidirectional Phase-shifted DC–DC Converter", *IEE Electronics Letters*, 1 April 1999, Vol. 35, No.7, pp. 523-524.

[6] Kazimierczuk M.K., Mescher M.J. and Prenger R.M., "Class D Current-Driven Transformer Center-Tapped Controllable Synchronous Rectifier", *IEEE Trans. on Circuits and Systems-I: Fundamental Theory and Applications*, Vol. 43, No. 8, August 1996, pp. 670-680.

[7] Yamashita N., Murakami N. and Yachi T., "Conduction Power Loss in MOSFET Synchronous Rectifier with Parallel-Connected Schottky Barrier Diode", *IEEE Trans. On Power Electronics*, Vol. 13, No. 4, July, 1998, pp. 667-673.